Luminescence spectroscopy of Mn^{2+} centres in rock-forming carbonates

G. WALKER, O. E. ABUMERE* AND B. KAMALUDDIN†

Dept. of Pure & Applied Physics, UMIST, Manchester M60 1QD

Abstract

Cathodoluminescence emission spectra and luminescence excitation spectra of Mn^{2+} in calcites, dolomites, magnesites, a manganocalcite and a rhodochrosite have been measured at both room temperature and 77 K. Ligand-field parameters have been calculated from the excitation spectra which reflect the size of the metal cation site in which the Mn^{2+} ion resides. The technique of luminescence excitation spectra has enabled the absorption profile of Mn^{2+} in Mg and Ca sites in dolomite to be separately determined. The variation of the distribution of Mn^{2+} between Mg and Ca sites in dolomites is demonstrated and discussed in terms of a simple model. It is concluded that the distribution of Mn^{2+} in dolomites may well provide information about its conditions of formation and/or subsequent alteration.

KEYWORDS: cathodoluminescence, manganese, carbonates, dolomite.

Introduction

IN recent years sedimentologists have been documenting the colour and intensity variations of cathodoluminescence in calcites and dolomites and correlating these with manganese and iron content (Machel, 1986; Fairchild, 1983; Frank et al., 1982; Pierson, 1981). Such cathodoluminescence indicators have been and are being used extensively in diagenetic studies to reveal information not readily obtained by other methods. It is generally accepted that the characteristic yellow-to-red cathodoluminescence of such minerals is due to emission from Mn^{2+} ions which are present in concentrations ranging from 10 ppm to around 1%. It is also found that an iron concentration in excess of about 1% has the effect of drastically reducing or extinguishing any such luminescence. Ten Have and Heijnen (1985) have shown the Mn^{2+} emission in calcite is visible at concentrations as low as 15–30 ppm provided the iron concentration is less than 200 ppm. There is, however, no reason why Mn^{2+} emission cannot be detected at even lower levels, provided the iron concentration is low and the detection system is of good enough sensitivity.

Cathodoluminescence colour and intensity variations are best investigated spectrally using photoelectric detection if the underlying causes are being sought, although in addition to, rather than in place of, visual or photographic observations; the geological context should, where possible, be recorded. However, surprisingly few spectral studies have been carried out, and those that have are mainly concerning synthetic calcites and dolomites rather than natural samples (Medlin, 1963, 1968; Sommer, 1972; Visokeras et al., 1973). Gies (1975) measured emission spectra of natural calcites under UV excitation (254 nm) and tried to correlate features with various impurities. However, UV is not very efficient in exciting Mn^{2+} emission unless sensitizers are also present, whereas electron-beam excitation usually produces intense Mn^{2+} emission. Aquilar and Osendi (1982) studied both the emission and excitation spectra of Mn^{2+} in calcite and also ascribed a UV emission to Mn^{2+} although Blasse and Aquilar (1984) subsequently suggested this emission was more likely to be due to Ce^{3+}.

In this paper we present a preliminary study of cathodoluminescence emission spectra and luminescence excitation spectra of calcites, dolomites, magnesites and rhodochrosite at room temperature, 77 K, and in some cases at even lower temperatures (7–10 K). Cathodoluminescence decay times have also been measured at various temperatures.

* Present addresses: *Physics Dept. University of Port Harcourt, Nigeria; †Physics Dept., University of Malaysia, Lembah Pentai, Kuala Lumpur, Malaysia.

Table 1. Ligand-field parameters for Mn^{2+} in carbonates, obtained from excitation spectra

	cation -anion distance (Å)	$10Dq(cm^{-1})$ $(\pm 200cm^{-1})$	$B(cm^{-1})$ $(\pm 20cm^{-1})$	$C(cm^{-1})$ $(\pm 50cm^{-1})$
calcite	2.36	7100	850	2950
magnesite	2.10	8500	840	2930
dolomite (Mg-site)	2.09	8500	840	2910
dolomite (Ca-site)	2.38	6600	850	2950
rhodo- chrosite	2.19	8300	800	3000*
mangano- calcite	-	7400	840	2950*

* Low temperature (7K) values

The free ion value B_0 of the Racah parameter $B = 910 cm^{-1}$.

The Trees correction coefficient α was taken as $76 cm^{-1}$.

Luminescence excitation spectra yield the absorption profiles of the luminescent species if absorption is direct (i.e. not via some other species). These spectra, therefore, show the bands associated with all the excited states of the luminescent ion and not just the emitting state as in emission spectra.

It is emphasized that these preliminary measurements are meant to form a basis for more detailed spectral studies of subtle CL colour variations of these minerals, particularly calcite and dolomite, in thin sections. Clearly, many outstanding problems will have to await the results of such studies where individual microscopic CL zones can be analysed spectrally. Nevertheless, the present work indicates what areas of study are likely to be fruitful.

Cation site symmetry and the Mn^{2+} emission

The size and symmetry of the metal cation site in which the Mn^{2+} ion finds itself affects not only the spectral position of the emission band but also the excitation spectra. Indeed, where there is more than one type of metal cation site, it is usually possible to determine whether the Mn^{2+} ion occupies both sites or has a strong preference for one particular type (Walker 1983, 1985).

The calcite group of minerals (which includes magnesite and rhodochrosite) has a rhombohedral structure, space group $R\bar{3}c$, and the unit cell contains two molecules. The essentially planar and triangular carbonate groups lie perpendicular to the three-fold axis. Each calcium (or other metal cation) is surrounded by six oxygen ligands in octahedral coordination; the octahgedron is,
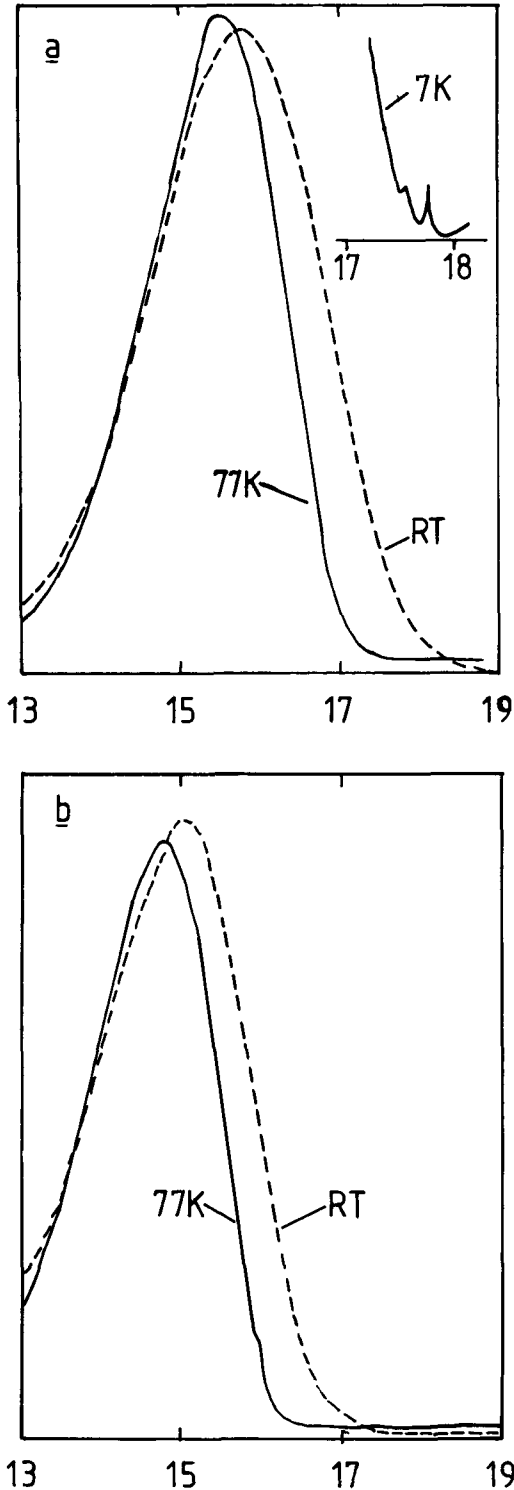
however, trigonally distorted, being slightly elongated along the above-mentioned triad axis, and lies between two carbonate planes. Although the site closely approximates to O_h symmetry, the actual point symmetry is D_{3d}. There are, therefore, six equal metal–oxygen distances (see Table 1) and the site remains strictly centrosymmetric.

The dolomite structure is slightly different in that magnesium and calcium atoms are ordered in alternate layers perpendicular to the principal axis, although in practice, the ordering and stoichiometry of Mg and Ca atoms is seldom perfect. Nevertheless, the Mg and Ca sites are quite different in size, the Mg site being slightly smaller than in magnesite and the Ca site slightly larger than in calcite (see Table 1). Both sites, however, once again remain centrosymmetric having S_6 point symmetry (Althoff, 1977; Beran and Zemann, 1977; Effenberger *et al.*, 1981).

The electronic transition responsible for luminescence in Mn^{2+} centres ($^4T_{1g}$–$^6A_{1g}$) is spin-forbidden but also, in the case of carbonates, Laporte forbidden for electric dipole transitions on account of the centre of symmetry; the same is true for transitions in absorption from the $^6A_{1g}$ ground state to the quartet excited states. Thus, a purely electronic transition involving no change in vibrational energy (i.e. a zero-phonon transition) would be expected to be a magnetic dipole transition which is Laporte allowed in a centrosymmetric site. Nevertheless, such a transition has a much lower probability than an electric dipole transition. However, electric dipole transitions would be spatially allowed (though still spin-forbidden) if vibronically coupled to a phonon mode of odd parity, i.e. to a vibrational mode of A_u or E_u symmetry. It is, therefore, likely that the Mn^{2+} emission in carbonates is mainly due to phonon-assisted electric-dipole transitions involving an A_u or E_u phonon mode. The spin-forbiddenness is broken down to some extent by a small degree of spin-orbit coupling, but the long decay times of Mn^{2+} luminescence and the weakness of the corresponding absorption transitions are a consequence of such forbiddenness (Walker, 1985).

Experimental

Cathodoluminescence was excited using a pulsed electron beam (10–15 keV; $1 \mu A \, mm^{-2}$) from a hot-cathode electron gun (Geake *et al.*, 1972). A large grating spectrometer with stepper-motor drive was used to scan the spectrum. Dispersed light was detected by a photomultiplier with an extended S20 response and lock-in amplification. The spectral data was then digitized, stored, corrected and plotted using a micro-

computer which was also used to control the spectrometer scanning. Signal averaging of multiple scans was also possible if the signal-to-noise ratio of a single scan proved unsatisfactory.

The sample, which was usually in microcrystalline powder form, could be placed on the cold finger of a continuous flow cryostat to permit measurements to be made at 77 K or at temperatures approaching liquid helium where necessary.

Chemical analyses of samples were by AAS using powders on which spectral measurements had been made. Cathodoluminescence decay curves were also determined at fixed wavelengths both at room temperature and 77 K using a boxcar detector. Luminescence excitation spectra were measured using a xenon arc source, grating spectrometer (as above) and photomultiplier. Similar data collection and scan control facilities were provided by the microcomputer as for emission spectra. In this technique, the integrated intensity of a particular luminescence band, isolated by a filter, is monitored as the wavelength of excitation is scanned. A 'double-chopper' technique is employed; the monochromatic excitation, and the weak luminescence emitted as a result are modulated in anti-phase, thereby preventing incident light scattered by the sample from reaching the photomultiplier. The chopping frequency required depends on the decay time of the emission. The actual experimental arrangement has been described elsewhere (Walker 1983, 1985). It can be shown that, when corrections are made for the variations in the incident light intensity, the spectral profile obtained is identical to the absorption spectrum of the luminescence species in the weak absorption limit (Hamilton et al., 1978). In fact, luminescence excitation spectra can yield absorption profiles in circumstances where conventional absorption spectroscopy is either very difficult or impossible. It can also circumvent the problem of overlapping absorption bands due to different absorbing species including the same ion (e.g. Mn^{2+}) in different sites (Walker 1983, 1985). In this paper, emission spectra are plotted in photons/sec/wavenumber intervals against wavenumber. For all spectra, wavenumber is preferred to wavelength since transition energies and band-

FIG. 1. Cathodoluminescence emission spectra of Mn^{2+} at room temperature (RT) and 77 K in (a) a typical calcite (Derbyshire) and (b) a typical magnesite (Austria). The inset (top right) in (a) shows phonon structure on the high-energy edge at 7 K. The ordinates are in relative units of photons/sec/wavenumber interval and the wavenumber scale is marked at 2000 cm^{-1} intervals. The spectra are corrected for the spectral response of the instrumentation.

widths can then be read-off directly. It should be remembered, however, that the shape of the spectrum will be somewhat different from that plotted in terms of wavelength and, indeed, the peak position of spectral bands will also be slightly different although such differences are small.

Spectral measurements

Cathodoluminescence emission spectra. Mn^{2+} luminescence in carbonates at room temperature invariably shows a broad bell-shaped band with a peak intensity in the range $14\,500$–$17\,000\,cm^{-1}$ (690–$590\,nm$). On cooling to $77\,K$ this band narrows, particularly on the high-energy side, and the peak shifts slightly to lower energies (longer wavelength).

In some minerals, e.g. forsterite (Green and Walker, 1985), sharp peaks appear on the high energy edge of the Mn^{2+} emission band at low temperatures. These are due to the purely electronic or zero-phonon transition (usually the sharpest and highest in energy) and its phonon replicas where one or more phonons of a particular dominant phonon mode are created during the emission of a photon. However, such phonon structure is not very evident in most carbonates, although some very weak fine structure can sometimes be detected at very low temperatures. The reason for the lack of prominent phonon structure at low temperatures is related to the degree of interaction between the electronic states of the Mn^{2+} ion and the vibrating lattice in which it finds itself. In the case of strong or moderately strong interaction, phonon structure is not evident (Walker, 1985; Imbusch, 1978).

Fig. 1*a* shows the emission spectrum of a typical calcite at room temperature and at $77\,K$. The maximum intensity is usually in the range $15\,800$–$16\,000\,cm^{-1}$, shifting to around $15\,500\,cm^{-1}$ at low temperatures. Careful correction for the spectral response of the instrumentation (photomultiplier response and spectrometer transmission) is essential for the accurate determination of the position of the band maximum. At $77\,K$ the full-width-at-half-maximum (f.w.h.m) of the emission band is about 0.8 of that at room temperature. Calculation shows that this implies that phonons with an average effective energy of around $300\,cm^{-1}$ are created during the emission process. In all probability, however, a number of phonon modes will be involved. The inset in Fig. 1*a* shows weak phonon structure on the high-energy edge at $7\,K$. If the sharp peak at about $17\,700\,cm^{-1}$ is the zero-phonon line then there is a first phonon replica $225\,cm^{-1}$ from it; this correlates with a known infra-red active mode of E_u symmetry (White,

1974). However, in many of the calcites studied this structure was not evident; some calcites (including some synthetic powder samples) also show emission bands which are some 10% broader at room temperature than that shown in Fig. 1*a*, and none of these exhibit phonon structure. The reason for this behaviour is not yet clear, but may be due to structural disorder.

Another possible cause of spectral broadening is microscopic CL zoning. Such CL zoning is well-known; variations from zone to zone may be simply of intensity. However, colour variations can be caused by varying proportions of two or more emission bands (e.g. blue and red bands). More subtly, the average environment of the Mn^{2+} ion in different zones may be slightly different as a result of different conditions of crystallization. Therefore, unless spectra of individual CL zones can be determined, the spectra obtained may be composites.

Spectra presented here are mainly from small powdered samples taken from single crystal calcites. Several samples were obtained from the same crystal which did not show appreciable variations in spectra. The conclusion must be that if CL zonation is present then the sample taken must be a consistent average of such zones.

The intensity of the Mn^{2+} emission in calcite is almost temperature independent between $7\,K$ and room temperature but the cathodoluminescence decay time increases appreciably on cooling from around 35–$40\,ms$ at room temperature to around $75\,ms$ at $77\,K$. Such a temperature dependence is characteristic of phonon-assisted transitions although the increase in decay time on cooling may also be due in part to phosphorescence involving electron trapping states. Decay curves are seldom simple exponential curves.

Although the effect of the presence of iron and other possible quenchers has not yet been addressed in the present work, it would clearly be interesting to see whether a decreased emission intensity attributed to the presence of iron was accompanied by an expected decrease in decay time.

In a typical magnesite, the Mn^{2+} emission appears at lower energies, the band peaking at about $15\,000\,cm^{-1}$ at room temperature and $14\,800\,cm^{-1}$ at $77\,K$ (see (Fig. 1*b*). Phonon structure is very difficult to detect even at liquid helium temperatures. The narrowing of the emission band on cooling and the intensity variation of the emission with temperature are both similar to calcite. It is, however, noticeable that Mn^{2+} emission in magnesite is usually less bright than in calcite. The difference between the Mn^{2+} emission band position in calcite and magnesite is mainly indica-
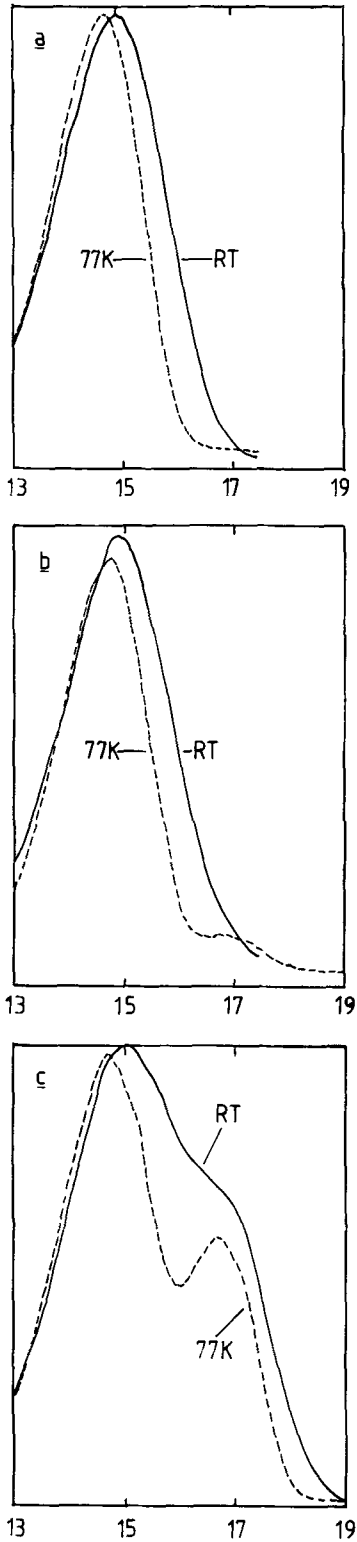
FIG. 2. Cathodoluminescence emission spectra of Mn^{2+} in dolomites at room temperature (RT) and 77 K: (a) a typical fine-grained sedimentary dolomite DMU5; (b) dolomite (Italy) BM37747; (c) dolomite (Zimbabwe) BM1933,448. See Fig. 1 caption for comments regarding scales, units and correction.

tive of the size of the metal cation site (see later discussion on dolomites).

Fig. 2 shows the cathodoluminescence emission spectra of three different dolomites. The most common types are those depicted in Figs. 2a and b where only a single band is clearly evident at room temperature. This band has a maximum at about $14\,900\,cm^{-1}$, shifting to around $14\,600\,cm^{-1}$ at 77 K, and is very similar to that in magnesite.

In Fig. 2b, a second band at higher energy becomes discernible at 77 K, owing mainly to the narrowing of the dominant red band. At first, calcite contamination might be suspected, but a comparison with typical calcite spectra shows that this smaller band is shifted to higher energies compared with the calcite emission. Fig. 2c shows the emission of a dolomite with more unusual CL characteristics in which this second band is apparent even at room temperature and is of comparable intensity to the red band. The cathodoluminescence of such dolomites is visually more yellow rather than red. The spectrum at 77 K shows the two band maxima well separated at about $14\,700\,cm^{-1}$ and $16\,700\,cm^{-1}$ respectively. By comparison with magnesite and calcite spectra, it seems probable that the red band is due to Mn^{2+} in Mg sites and the yellow band to Mn^{2+} in Ca sites. Later we shall see that luminescence excitation spectra of these bands demonstrate beyond doubt that this interpretation is correct. The distribution of Mn^{2+} between Mg and Ca sites has been the subject of much discussion and we shall return to this problem later.

Many carbonates also often show a weaker blue cathodoluminescence band, particularly at low temperatures. This band, which is very broad, is in many ways similar to that often seen in many silicates and probably involves a similar intrinsic lattice defect. However, to return to manganese centres, in most natural carbonates, manganese is present in concentrations usually much less than 1%. It is, therefore, interesting to see what happens when the manganese content is much higher. A manganocalcite (14.9% MnO) and a rhodochrosite (59% MnO) were, therefore, studied for the purposes of comparison. Cathodoluminescence emission spectra are shown in Fig. 3. It can be seen that the manganocalcite emission band is shifted slightly to lower energies (max. $15\,225\,cm^{-1}$ at 77 K) compared with calcite as might be expected (Mn^{2+} being smaller than Ca^{2+}). It is luminescent at room temperature but has a decay time noticeably shorter (10 ms) than in calcite. However, as the temperature is decreased the luminescence intensity increases, slowly at first, but then quite rapidly. At 77 K it has increased by a factor of 2 or more and is
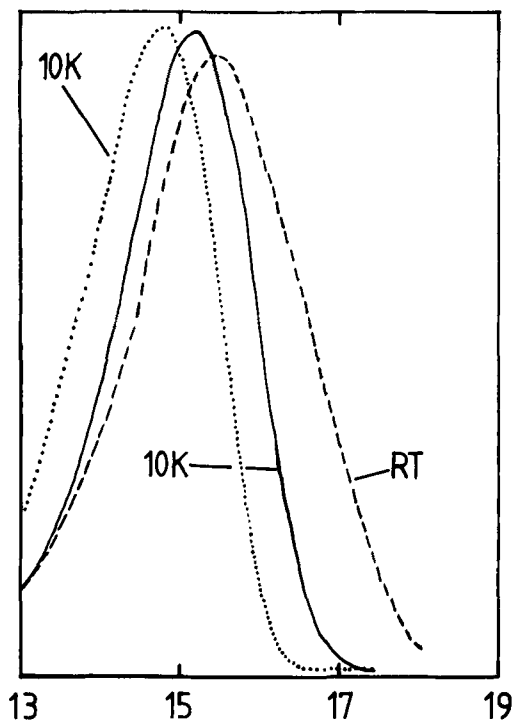

FIG. 3. Cathodoluminescence emission spectra of Mn^{2+} in a manganocalcite (Broken-Hill, Australia) at room temperature (RT) and 10 K (continuous line) and a rhodochrosite (dotted line) at 10 K. The origin of the rhodochrosite is not known. See Fig. 1 caption for comments regarding scales, units and correction.

still increasing. The decay time at 77 K has increased to about 30 ms.

Rhodochrosite is virtually non-luminescent at room temperature but exhibits a bright red luminescence at very low temperatures (below 77 K). The emission spectrum in Fig. 3 is much closer to that of magnesite rather than that of calcite. At temperatures in the range 100–5 K, the emission intensity increases rapidly, by almost 50-fold, with decreasing temperature. At 77 K the decay time is about 15 ms. The luminescence of Mn compounds such as rhodochrosite is of special interest since, according to the theory expounded by Imbusch (1978), the Mn^{2+} ions responsible for the emission are centres perturbed by the presence of an adjacent impurity or defect. Since rhodochrosite usually contains small amounts of Ca and Mg as well as Fe (AAS analysis of the rhodochrosite studied was 0.66% CaO, 0.8% MgO and 1.3% FeO by weight), the emitting centre may well be adjacent to such a Ca^{2+} or Mg^{2+} ion. In fact, the excitation energy of a 'normal' Mn^{2+} ion will 'hop' rapidly from one ion to another until

it becomes trapped on a perturbed Mn^{2+} ion or until the energy becomes transferred to a similar ion such as Fe^{2+}. If the latter occurs then quenching will result and, at room temperature, this is what normally happens since the perturbed Mn^{2+} traps are rapidly emptied thermally before emission can take place. However, at lower temperatures the emptying of such traps becomes much less efficient and the probability of emission from perturbed Mn^{2+} ions becomes high. The emission spectrum is probably characteristic of such perturbed ions, rather than the majority of 'normal' Mn^{2+} ions.

In the manganocalcite, where about one in four metal cations are Mn^{2+}, nearest-neighbour cations will include both Mn^{2+} and Ca^{2+} and, therefore, energy transfer between Mn^{2+} ions is again very probable. The ratio of nearest-neighbour Ca^{2+} to Mn^{2+} ions is, however, likely to be variable resulting in Mn^{2+} centres of slightly different energies which once again would create shallow traps. The manganocalcite studied also contained 0.04% MgO by weight (AAS analysis) and Mg^{2+} ions may also perturb the energy levels of an adjacent Mn^{2+} ion. Hence, quenching is enhanced at room temperature due to energy transfer to Fe^{2+} ions (in this case AAS analysis gave a FeO content of 0.65% by weight) but is less effective at low temperatures where energy trapping by Mn^{2+} ions with excited states of lower than average energy is more probable.

Luminescence excitation spectra. Fig. 4a and b show the luminescence excitation spectra of the Mn^{2+} emission bands of a typical calcite and magnesite respectively; these characteristic d^5 ligand-field spectra are unequivocal proof, if such is needed, of the origin of the emission bands. From these spectra, the ligand-field strength 10 Dq and the electron repulsion parameters (Racah parameters B and C) can be found and the values calculated from Trees-corrected, cubic weak-field matrices are given in Table 1. However, more simply, a brief comparison of band positions in Fig. 4a and b shows the lower energy bands $^4T_{1g}$ and $^4T_{2g}(G)$ shifted further to lower energies in the stronger ligand field of the Mg site in magnesite than in the weaker field of the Ca-site in calcite. For reasons connected with the interference of bands at higher energies due to other centres, the best spectra are obtained at room temperature. However, the lowest energy band, due to the $^6A_{1g}$–$^4T_{1g}$ transition (which is the reverse of the transition causing luminescence emission), was studied at 77 K and 7 K to search for phonon structure; unfortunately none could be detected and the identification of the $17\,700\,cm^{-1}$ sharp peak, detected in the emission of some calcites
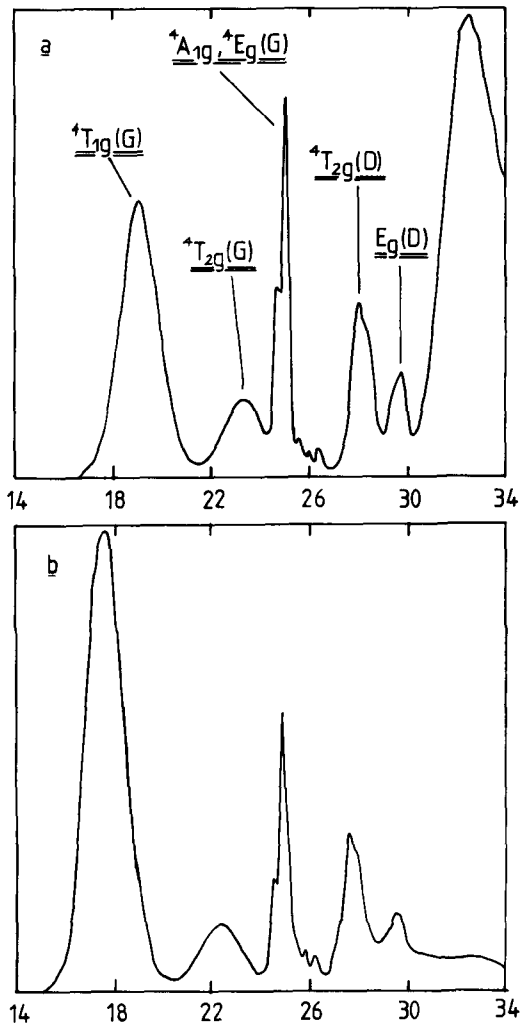

FIG. 4. Luminescence excitation spectra of the Mn^{2+} emission bands at room temperature in (a) a typical calcite (Derbyshire) and (b) a typical magnesite (Austria). Ordinates are in relative units of absorption coefficient and the wavenumber scale is marked at $4000\,cm^{-1}$ intervals. All spectra are corrected for variations in excitation intensity. Wratten 16 and 29 filters were used to isolate the emission bands in (a) and (b) respectively.

as a zero-phonon transition, could not, therefore, be proved. (Zero-phonon transitions occur in the same spectral position in emission and absorption or excitation.)

The sharp ligand-field independent $^4A_{1g}$, ^4E_g states appear to have some small fine structure on the high-energy side, even at room temperature. The zero-phonon transitions to the $^4A_{1g}$, ^4E_g states are likely to be of magnetic-dipole character due to the centre of symmetry. However, phonon-
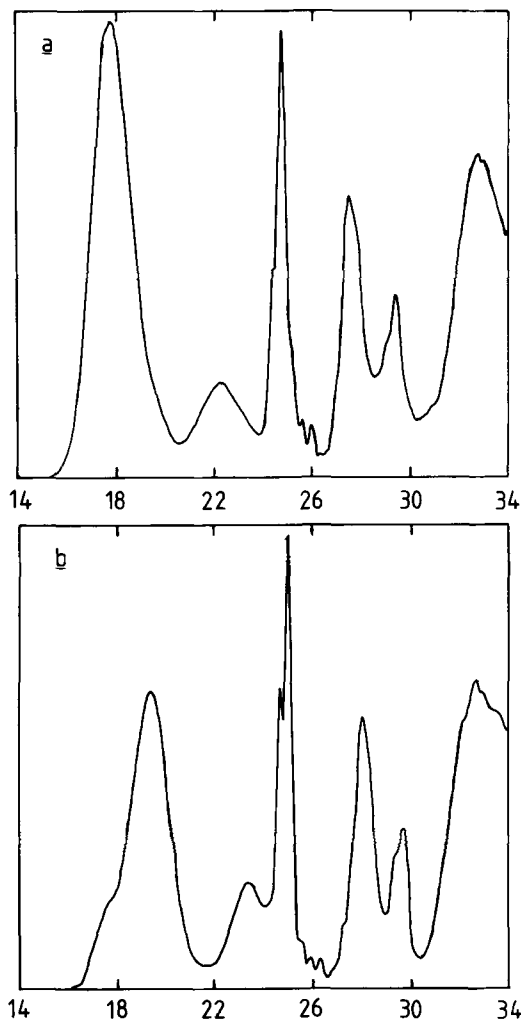
FIG. 5. Luminescence excitation spectra of Mn^{2+} at room temperature in (a) the Mg site and (b) the Ca site of dolomite BM1933,448. A Wratten 70 filter and a photomultiplier with an extended S20 response (red sensitive) was used for spectrum (a) and a Wratten 16 filter and a photomultiplier with an S11 response (red insensitive) for spectrum (b). The shoulder on the low-energy side of the lowest $^4T_{1g}$ band at around 18,000 cm^{-1} in spectrum (b) shows that a little of the $^4T_{1g}$ band of spectrum (a) is still present due to some residual red response of the S11 photomultiplier; additional filtering removes it but attenuates the signal to an undesirable extent. See Fig. 4 captions for other comments.

assisted electric dipole transitions to certain vibrational levels of these states are probable (see earlier) and this fine structure may be due to such transitions, although it is unusual to see such structure at room temperature.

The intense band at around 32 500 cm^{-1} in the calcite spectrum is in the region where the $^4T_{1g}(P)$ state would be expected. However, there is no such corresponding band in the magnesite spectrum. Moreover, this band in some calcites can be an order of magnitude more intense than that shown in Fig. 4a and can mask the $^4E_g(D)$ state. It is also often present in the spectra of Mn^{2+} in dolomites, where it appears in approximately the same spectral position (see Fig. 5). Its origin, therefore, is probably not due to Mn^{2+} but to an absorbing species which transfers its excitation energy to Mn^{2+}, i.e. a sensitizer. Since the band does not appear in the spectrum of Mn^{2+} in magnesite, it is probably due to a sensitizer ion substituting for Ca. A very similar band was found in calcite by Aquilar and Osendi (1982) which was later ascribed to Ce^{3+} by Blasse and Aquilar (1984).

Fig. 5a and b show the excitation spectra of the two emission bands of a dolomite which were shown in Fig. 2c. The separation of these two overlapping bands by means of available filters is difficult but, as can be seen, achievable; the experimental details are given in the figure caption. Here we see the separate absorption profiles of the Mn^{2+} ion in (a) an Mg site and (b) in the Ca-site in this particular dolomite; such a separation of absorption bands can only be achieved by using this powerful luminescence technique. The excitation spectra of red emission band of the dolomites in Fig. 2a and b are not shown but are very similar to Fig. 5a, and this in turn is similar to that of the magnesite in Fig. 4b. On the other hand the spectrum in Fig. 5b is more nearly like that of calcite in Fig. 4a, although the positions of the bands are slightly different. Values of 10 Dq, B and C for Mn^{2+} in the two metalcation sites in dolomite are given in Table 1.

Fig. 6a and b show the luminescence excitation spectra of the emission bands of rhodochrosite and manganocalcite shown in Fig. 3. These were measured at very low temperatures where the emission intensity was strongest. The ligand-field parameters from these spectra are given in Table 1 but it must be borne in mind that these have been evaluated from low-temperature spectra; values of 10 Dq might thus be expected to be slightly larger, and Racah parameters slightly smaller, than at room temperature. Although the emission from rhodochrosite is expected to be from 'perturbed' Mn^{2+} ions, the absorption will be dominated by that of 'normal' Mn^{2+} ions, so that the values of 10 Dq, B and C will be those appertaining to 'normal' Mn^{2+} ions. The sharpness of the spectral features in the rhodochrosite spectrum is notable and is thought to be due to
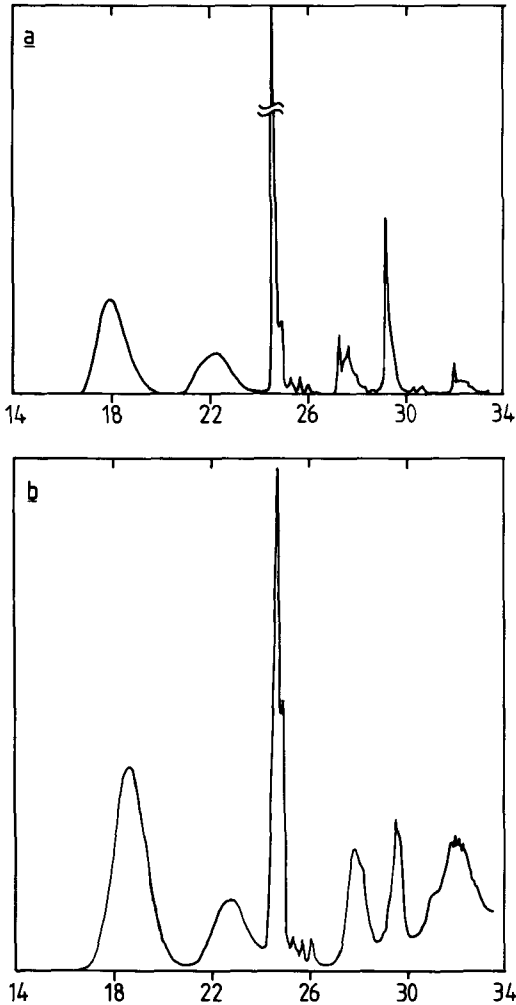
FIG. 6. Luminescence excitation spectra of Mn^{2+} at 7 K in (a) a rhodochrosite and (b) a manganocalcite. Note that in the rhodochrosite spectrum the ligand-field independent bands $^4A_{1g}$, $^4E_g(G)$ and $^4E_g(D)$ become very sharp and very intense due to the breakdown of spin forbidden state resulting from Mn–Mn interaction, which is also happening to a more limited extent in the manganocalcite spectrum. Wratten 29 and 25 filters were used for spectrum (a) and (b) respectively. See Fig. 4 caption for other comments.

spin-exchange interactions between Mn^{2+} ion pairs. However, this aspect and the spectra of such concentrated Mn systems in general will be discussed elsewhere.

The manganocalcite spectrum (Fig. 6b) is, not surprisingly, similar to that of calcite with the $^4T_{1g}(G)$ bands shifted to somewhat lower energies. The most notable difference is the reversal of intensity between the sharp $^4A_{1g}$ and $^4E_g(G)$ bands which also occurs to a more dramatic extent in rhodochrosite.

It is noteworthy that excitation spectra of all the carbonates investigated show no appreciable splitting of the ligand-field states of Mn^{2+} in contrast to that evident in enstatite and forsterite (Walker, 1985). Thus the distortion of the occupied sites from O_h symmetry must be comparatively small.

Discussion: Mn^{2+} site occupancy in dolomites

Perhaps the most immediate application of the results of this work concerns the spectra of dolomites, in particular the Mn^{2+} spectra in Mg and Ca sites and the variability of the partitioning of Mn^{2+} ions between these sites. It can be seen from Table 1 that there is little or no discernible difference in the ligand-field parameters between Mn^{2+} in the Mg site in dolomite and that in magnesite. The fact that the emission in dolomite is usually at a slightly lower energy than that in magnesite is due more to a slightly larger Stokes shift between absorption and emission in dolomite rather than to a larger ligand field. (This does not, however, mean that the excitation spectra are identical; there are subtle differences in band positions, and dolomites usually show a sensitizer band at around $32\,500\,cm^{-1}$). On the other hand, the ligand-field strength $10\,Dq$ for Mn^{2+} in the Ca site in dolomite is noticeably different from that in calcite.

The preference of Mn^{2+} for the smaller Mg site in most dolomites is now well-documented experimentally, by both luminescence and electron spin resonance (ESR) measurements (Wilderman 1970; Lumsden and Lloyd, 1984). These results are noticeably different from luminescence (Walker 1983, 1985) and ESR measurements (Gaite, 1975) on Mn^{2+} in diopside, where a similarly small Mg site and a larger Ca site are comparably populated.

Wildeman (1970) found that in sedimentary dolomites the ratio of Mn^{2+} in Mg/Ca sites was about 4:1, whereas, in some hydrothermally altered dolomites it was much higher. More recently, Lumsden and Lloyd (1984) found a correlation between a non-stoichiometric excess of Ca of between 1 and 5% and a Mg/Ca site population ratio for Mn^{2+} of about 5, whereas more stoichiometric dolomites had a much higher ratio (up to 70). They also noted that dolomites from core samples of the Deep Sea Drilling Project either gave 'smeared' ESR patterns or indicated an Mn^{2+} population ratio of around unity or less.

The obvious question is whether the usual

strong preference of Mn^{2+} for the Mg site in dolomite is to be expected on theoretical grounds. Since in its high-spin state the Mn^{2+} ion has a half-filled d-shell, ligand-field effects do not influence its site preference. Moreover, the major difference between the Mg and Ca site is one of size rather than symmetry, although ESR measurements suggest that the Mg site is usually distorted more than the Ca site by Mn^{2+} occupation. As already mentioned, optical spectra suggest that such distortion is not large. Detailed lattice energy calculations of the type carried out by Catlow et al. (1982) may provide an answer.

However, a simplistic model for Mn^{2+} distribution in dolomites has been suggested by Kretz (1982). This model relates the distribution to the residence time of the Mn^{2+} in Mg and Ca sites during crystal growth at around 650 °C; these residence times are assumed to be proportional to the differences between the ionic radii of Mn^{2+} and Mg^{2+} or Ca^{2+}. It predicts that there should be about 1.5 times more Mn^{2+} ions in Mg sites than Ca sites which is remarkable considering the nature of the assumptions made. More realistically, the residence time in a particular site is likely to be related to the binding energy E by a Boltzmann factor $\exp(-E/kT)$. If the potential energy curve is assumed to be parabolic then E will depend on the square of the difference in ionic radii or cation–anion distances. However, the size of the constant of proportionality which determines the 'width' or curvature of the parabolic potential curve is not known. Furthermore, the precise form of the potentials energy vs. cation–anion distance curve may not be parabolic for Mn^{2+} octahedrally co-ordinated by oxygen ligands in carbonates. Nevertheless, the curve is likely to have a roughly similar shape to a Morse potential and is shown schematically in Fig. 7. Here the energy difference ΔE is that between an Mn^{2+} ion in a magnesium site and Mn^{2+} in a calcium site. The population ratio is then $\exp(\Delta E/kT)$ where T (K) is the absolute temperature of formation or that at which appreciable ion diffusion has taken place. If, for example, $\Delta E = 2kT$ the Mg/Ca site population ratio would be about 7 and even at 650 °C, $2kT$ is only around 0.15 eV.

The effect of a small variation in the cation–anion distances can be readily seen. For example, high pressure would tend to reduce cation–anion distances and thereby decrease ΔE, resulting in a smaller Mg/Ca population ratio at a particular temperature (T).

The effect of the temperature of formation on Mn^{2+} distribution is rather more difficult to predict since both ΔE and kT would decrease with
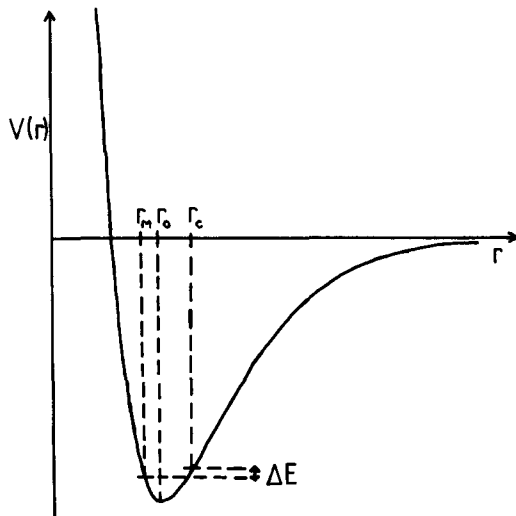

FIG. 7. Schematic diagram of the probable potential energy $V(r)$ vs. r (cation–anion distance) curve for Mn^{2+} in octahedral coordination by oxygen ligands in carbonates. r_o is the cation–anion distance for minimum energy and corresponds approximately to that which exists in rhodochrosite. r_m and r_c are the cation–anion distances for Mn^{2+} in the Mg site and Ca-site respectively in dolomite. ΔE is the energy difference between Mn^{2+} in a Ca-site and that in a Mg site in dolomite.

decreasing temperature. Although experimentally the most common Mg/Ca site population ratio appears to be about 5, there can be a very large variation in this figure. In view of this variation, it is clear that the difference in lattice energy between placing Mn^{2+} ions in Mg sites and placing them in Ca sites must be relatively small and that differences in conditions of formation and/or subsequent alteration can cause the balance between Mg and Ca site population to be tilted one way or the other.

Conclusions

It is clear that cathodoluminescence can provide a simple means of recognizing dolomite phases with appreciable Ca-site populations by Mn^{2+}. The possibility of using the distribution of Mn^{2+} ions in dolomite as an indicator of conditions of formation or alteration, as suggested by Lumsden and Lloyd (1984), appears feasible. There is already evidence that dolomites formed at, or subjected to, high pressure show appreciable Ca-site population by Mn^{2+}. The question is what other possible conditions of formation, if any, would result in similar Mn^{2+} distributions.

Acknowledgements

References

Althoff, P. L. (1977) *Am. Mineral.* **62**, 772–83.

Aquilar, G. M. and Osendi, M. I. (1982) *J. Luminescence*, **27**, 365–75.

Beran, A. and Zemann, J. (1977) *Tscherm. Mineral. Petr. Mitt.* **24**, 279–86.

Blasse, G. and Aquilar, M. (1984) *J. Luminescence*, **29**, 239–41.

Catlow, C. R. A., Thomas, J. M., Parker, S. C. and Jefferson, D. A. (1982) *Nature*, **295**, 658–62.

Effenberger, H. K., Mereiter, K. and Zemann, J. (1981) *Z. Kristallogr.* **156**, 233–43.

Fairchild, I. J. (1983) *Sedimentology*, **30**, 579–83.

Frank, J. R., Carpenter, A. B. and Oglesby, T. W. (1982) *J. Sediment. Petrol.* **52**, 631–8.

Gaite, J. M. (1975) *J. Phys. C.* **8**, 3887–95.

Geake, J. E., Walker, G., Mills, A. A. and Garlick, G. F. J. (1972) *Proc. 3rd Lunar Sci. Conf., Geochim. Cosmochim. Acta. Supple. 3*, **3**, 2265–75.

Gies, H. (1975) *Mineral. Deposita*, **10**, 216–27.

Green, G. R. and Walker, G. (1985) *Phys. Chem. Minerals*, **12**, 271–8.

Hamilton, T. D. S., Munro, I. H. and Walker, G. (1978) In *Luminescence Spectroscopy* (Lumb, M. D., ed.) Academic Press, London, pp. 149–283.

Imbusch, G. F. (1978) Ibid. pp. 1–92.

Kretz, R. (1982) *Geochim. Cosmochim. Acta*, **46**, 1979–81.

Lumsden, D. N. and Lloyd, R. V. (1984) Ibid. **48**, 1861–5.

Machel, H. G. (1986) *Geoscience Canada*, **12**, 139–47.

Medlin, W. L. (1963) *J. Opt. Soc. Am.* **53**, 1276–85.

——(1968) In *Thermoluminescence of Geological Materials* (McDougall, D. J., ed.) Academic Press, London and New York, pp. 193–223.

Pierson, B. J. (1981) *Sedimentology*, **28**, 601–10.

Sommer, S. E. (1972) *Chem. Geol.* **9**, 257–73.

Ten Have, T. and Heijnen, W. (1985) *Geologie Mijnbouw*, **64**, 297–310.

Visokeras, R., Ceva, T., Lapraz, D., Iacconi, P. and Lefaucheux, F. (1973) *Phys. Stat. Solidi (a)*, **15**, 61–6.

Walker, G. (1983) *Chem. Britain*, **19**, 824–31.

——(1985) Mineralogical applications of luminescence techniques. In *Chemical Bonding and Spectroscopy in Mineral Chemistry* (Berry, F. J. and Vaughan, D. J., eds.) Chapman & Hall, London, pp. 103–40.

White, W. B. (1974) The Carbonate Minerals. In *The Infra-Red Spectra of Minerals* (Farmer, V. C., ed.) Min. Soc. London, U.K.

Wildeman, T. R. (1970) *Chem. Geol.* **5**, 167–77.